ChemComm

Check for updates

A synthesis-enabled relative configurational assignment of the C31–C46 region of hemicalide†

Tegan P. Stockdale, Nelson Y. S. Lam [ID] * and Ian Paterson [ID] *

With 21 unknown stereocentres embedded in spatially separated stereoclusters, the cytotoxic polyketide hemicalide represents a seemingly intractable structural assignment problem. Herein, through the targeted synthesis of configurationally defined fragments, as well as "encoded" mixtures of diastereomers, the stereochemical elucidation of the C31–C46 region of hemicalide is achieved. Detailed NMR spectroscopic analysis of candidate fragments and comparison with the related hemicalide data strongly supported a 31,32-*syn*, 32,36-*anti* and 42,46-*anti* relationship. In combination with previous work on hemicalide, this reduces the number of possible structural permutations down to a more manageable eight diastereomers.

Hemicalide (**1**, Fig. 1) is a complex polyketide isolated from the marine sponge *hemimycale sp.*, exhibiting extraordinary pico-molar IC$_{50}$ values against a panel of human cancer cell lines through a putative antimitotic mode of action.[1] First reported in the patent literature in 2011, all 21 stereocentres within hemicalide were initially unassigned, leaving over two million possible permutations.

By interrogation of the available ^{1}H and ^{13}C NMR data for hemicalide, our group along with that of Ardisson–Meyer–Cossy have focused on solving this challenging stereochemical conundrum through the synergistic combination of synthetic and computational approaches. To date, this has enabled the confident assignment of the C8–C13 stereohexad,[2,3] C18–C24 dihydroxylactone[4] and C36–C42 hydroxylactone regions.[5,6] In addition, a synthesis-enabled investigation established the relative configuration between the C8–C13 and C18–C24 regions.[7] These cumulative efforts served to narrow the possible structural permutations down to 128 stereoisomers, leaving the C27–C32 stereotetrad, the isolated C45 stereo centre, as well as their relationship to the other stereoclusters, unassigned.[8–10]

Yusuf Hamied Department of Chemistry, Lensfield Road, Cambridge, CB2 1EW, UK
† Electronic supplementary information (ESI) available: Full experimental and characterisation details; NMR correlation tables and bar graphs. See DOI: **https://doi.org/10.1039/d2cc01802k**
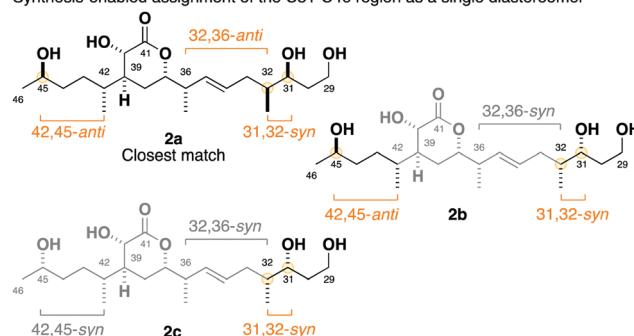
Herein, we report a targeted synthesis of the C35–C43 region of hemicalide and its elaboration to generate the candidate fragments **2a**, **2b** and **2c**. Detailed NMR spectroscopic comparison with the natural product then served to assign the previously unknown C31, C32 and C45 stereocentres relative to the C35–C43 region. Through this evolutionary approach,[11,12] the C31–C46 region is narrowed down to a single diastereomer, translating to only eight possible diastereomers remaining for hemicalide.

Seeking flexibility in the installation of the C45 hydroxyl-bearing stereocentre, as well as modularity in appending
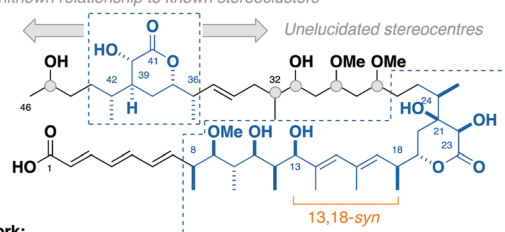
Fig. 1 Structure of hemicalide (**1**) and the assigned relative configurations of each region determined to date. Through the stereocontrolled synthesis of the candidate truncate fragments **2a**, **2b** and **2c**, followed by detailed ^{1}H and ^{13}C NMR correlations, this work assigns the C31–C46 region as a single diastereomer as in **2a**.
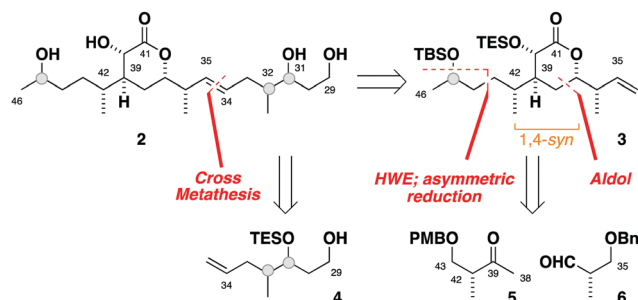
Fig. 2 Retrosynthesis for the C29–C46 truncate **2**.

candidate C29–C34 fragments, **2** was disconnected across the internal C34–C35 alkene to afford the terminal alkenes **3** and **4** (Fig. 2).[13] Given the isolated nature of C45, we planned to perform a stereoselective carbonyl reduction of the corresponding enone under reagent control followed by hydrogenation. Recognition of the 1,4-*syn* relationship between C37 and C42 alluded to the execution of a boron-mediated aldol reaction between the Roche ester-derived building blocks **5** and **6**. Critically, the antipode of **3** could then be readily obtained by using the enantiomeric components.

Synthesis of the alkene **3** commenced with a (+)-Ipc$_2$BCl mediated aldol reaction between the known ketone **5**[4] and the aldehyde **6**[14] to afford **7** (>20:1 dr),[15] following silyl ether formation (Scheme 1). Preliminary studies towards installing the C39 stereocentre *via* the conjugate reduction of a cyclic enoate derivative afforded the undesired configuration,[16] indicating that a suitable *acyclic* enoate might be sought. To this end, a tandem aldol reaction on the ketone **7** using the lithium enolate of **8**, followed by *in situ* Peterson olefination gave the Z-enoate **9**. Extensive experimentation revealed that the desired C39 configuration was best installed through a hydroxyl-directed reduction under optimised conditions. Thus, following silyl ether cleavage of **9**, hydrogenation of the resulting alkene **10** mediated by Crabtree's catalyst ([Ir(cod)py(PCy$_3$)] [PF$_6$], 13 mol%, H$_2$, 1 atm) at low temperature (−23 °C) and acidic workup delivered the δ-lactone **11** (5:1 dr) now favouring the desired C39 configuration.[17] From **11**, α-hydroxylation *via* reaction of the derived potassium enolate with Davis oxaziridine[18] cleanly gave the alcohol **12** (>20:1 dr) bearing the required C40 configuration.[5] Silyl ether formation then enabled the chromatographic separation of the C39 epimers to obtain the desired C35–C43 fragment **13**.

From **13**, a sequence of PMB ether cleavage, followed by oxidation of the resulting alcohol to the aldehyde and Horner–Wadsworth–Emmons (HWE) olefination cleanly delivered the requisite *E*-enone **14**.[19] A preliminary screen revealed that the flexible installation of the C45 stereocentre was achievable under Terashima asymmetric reduction conditions, with either C45-configuration (42,45-*anti* **15** and 42,45-*syn* **16**) selectively obtained (6:1 dr) through use of the appropriate antipode of the *N*-methylephedrine ligand.[20]

Preliminary reconnaissance next revealed that the C45 alcohol was best derivatised as its TBS ether to avoid any desilylation under subsequent hydrogenation conditions. In a parallel
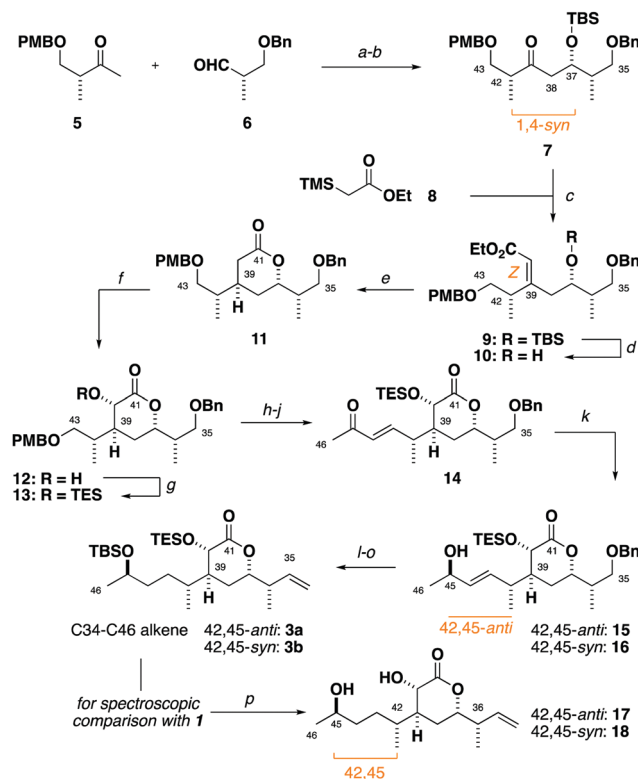
Scheme 1 Synthesis of hemicalide C34–C46 alkenes **3a** and **3b**, and fragments **17** and **18** for the spectroscopic determination of the C45 relative configuration. *Reagents and conditions*: (a) **5**, (+)-Ipc$_2$BCl, Et$_3$N, Et$_2$O, 0 °C; **6** −78 → −20 °C, 91%, >20:1 dr; (b) TBSOTf, 2,6-lutidine, CH$_2$Cl$_2$, −78 → 0 °C, 99%; (c) **8**, LDA, THF, −78 °C; **7**, THF, −78 °C → rt, 80%, >19:1 Z:E; (d) TsOH·H$_2$O, MeOH, rt, 97%; (e) [Ir(cod)py(PCy$_3$)][PF$_6$] (13 mol%), H$_2$ (1 atm), CH$_2$Cl$_2$, −20 °C → rt; TsOH·H$_2$O, 93%, 5:1 dr; (f) **11**, KHMDS, THF, −78 °C; 2-phenylsulfonyl-3-phenyloxaziridine, THF, −78 °C, 81%, >20:1 dr; (g) TESOTf, 2,6-lutidine, CH$_2$Cl$_2$, −78 °C, >99%; isolated 37,39-*anti* diastereomer: 85%; (h) DDQ, CH$_2$Cl$_2$/pH 9.2 buffer (4:1), rt, 97%; (i) (COCl)$_2$, DMSO, CH$_2$Cl$_2$; Et$_3$N, −78 → −20 °C; (j) dimethyl 2-oxopropylphosphonate, Ba(OH)$_2$, THF/H$_2$O (40:1), 0 °C → rt, 74% over two steps, >20:1 E:Z; (k) For **15**: LiAlH$_4$, (+)-*N*-methylephedrine, *N*-ethylaniline, Et$_2$O; −94 °C, 62%, 6:1 dr; (l) TBSOTf, 2,6-lutidine, CH$_2$Cl$_2$, −78 °C, 92%; (m) RANEY® Ni, H$_2$, EtOAc, rt, 99%; (n) Dess–Martin Periodinane, NaHCO$_3$, CH$_2$Cl$_2$, rt; (o) MePPh$_3$Br, *n*BuLi, THF, 0 °C → rt, 81% over two steps; (p) HF·py, py, THF, 0 °C, 99%.

sequence, concomitant alkene hydrogenation and benzyl ether cleavage with RANEY® nickel, oxidation and Wittig methylenation afforded both candidate fragments of the full C34–C46 alkene (42,45-*anti* **3a**, 42,45-*syn* **3b**) in readiness for the downstream cross metathesis for chain extension.

At this stage, global desilylation permitted a head-to-head NMR spectroscopic comparison with hemicalide, enabled by the timely provision of the original FID files by the isolation team (Table 1). Interrogation of the ¹H and ¹³C chemical shift data for the epimeric fragments **17** and **18** indicated that **17** containing a 42,45-*anti* relationship (entry 1: Σ|Δ$_H$| = 0.05 ppm; Σ|Δ$_C$| = 0.38 ppm) was a closer fit to the natural product than the alternative 42,45-*syn* configuration present in **18** (entry 2: Σ|Δ$_H$| = 0.13 ppm; Σ|Δ$_C$| = 0.67 ppm).

At this juncture, we undertook the detailed spectroscopic analysis of a reported full skeletal structure of hemicalide

Table 1 Determination of the 42,45-*anti* configuration in hemicalide. Statistical summary of absolute errors $|\Delta|$ (ppm)[ab] in **17** and **18** compared to the reported ^{1}H and ^{13}C NMR chemical shift data (ref. 1) for the corresponding region in hemicalide (**1**)
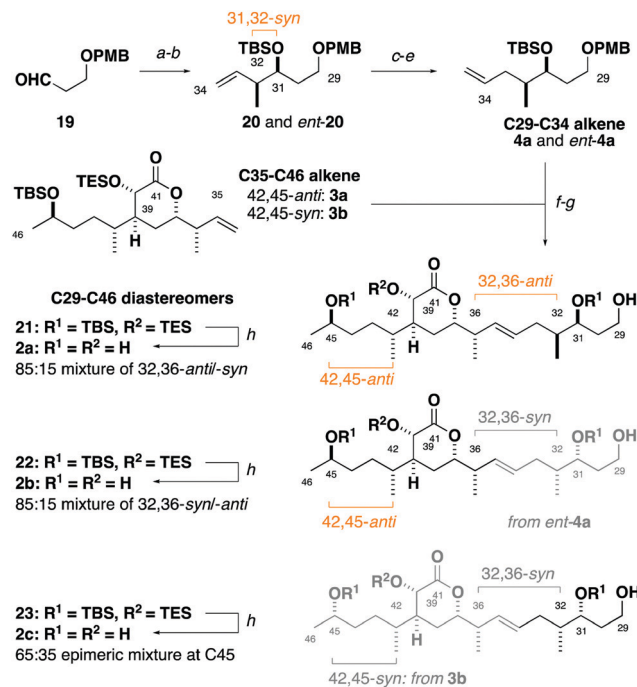
Entry	Sum $|\Delta|$ [1]H	Max $|\Delta|$ [1]H	Sum $|\Delta|$ [13]C	Max $|\Delta|$ [13]C
1. 42,45-*anti* **17**	**0.05**	**0.02**	**0.38**	**0.10**
2. 42,45-*syn* **18**	0.13	0.05	0.67	0.20

[a] Absolute errors taken for NMR shifts between H/C39-H/C46. [b] $|\Delta| = \delta$(experimental shift) − δ(reported shift), errors in ppm.

bearing a 31,32-*anti* configuration,[9] noting significant ^{1}H and ^{13}C NMR chemical shift deviations in this region *vis-à-vis* the natural product (Fig. 3). This provided strong evidence against a 31,32-*anti* relationship and gave us confidence to concentrate on the alternative and unconsidered 31,32-*syn* configuration.

Synthesis of the C29–C35 alkene fragment commenced with a Brown *syn*-crotylation of the aldehyde **19**[21] and silylation to afford the TBS ether **20** and set the 31,32-*syn* configuration (Scheme 2).[22] Alkene hydroboration, alcohol oxidation and Wittig methylenation then provided the homologated alkene **4a**. An analogous sequence using the enantiomeric crotylation reagent delivered *ent*-**4a** as required to establish the relationship between the stereoclusters. From here, a parallel cross-metathesis with **3a** (containing the 42,45-*anti* configuration) mediated by Hoveyda–Grubbs II catalyst (13 mol%), followed by PMB ether cleavage, gave the separate C29–C46 fragments 32,36-*anti* **21** and 32,36-*syn* **22**.[23] Global desilylation under fluorous conditions then gave the truncated tetraols **2a** and **2b** for detailed NMR spectroscopic comparison. An analogous sequence with **3b** (42,45-*syn* configuration) and *ent*-**4a** provided the 32,36-*syn*, 42,45-*syn* diastereomer **2c**.
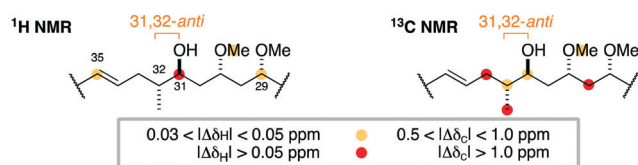
At the outset, we were cognisant that subtle and minute chemical shift differences resulting from 1,4- and 1,5-related stereoclusters separated by flexible acyclic linkers could confound conclusions in this study. This was anticipated for the as yet unassigned stereocentres at C31, C32 and C45 in the sidechains appended to the established δ-lactone region. To ameliorate this, we prepared fragment **2c** bearing the 32,36-*syn*, 42,45-*syn* configuration containing an "encoded" 65:35 epimeric mixture at C45, as well as a configurationally pure C35–C46 region coupled with an "encoded" 85:15 mixture of the C29–C35 alkene enantiomers to generate **2b** as an 85:15 mixture of 32,36-*syn* and -*anti* diastereomers. Analogously, **2a** was synthesised containing an 85:15 mixture of 32,36-*anti* and -*syn* diastereomers with **2b** as the minor component (see the ESI†).[24] With these fragments in hand, detailed ^{1}H and [13]C

Fig. 3 Comparison of the ^{1}H and ^{13}C NMR chemical shifts for the C29–C35 region of a previously reported diastereomer (ref. 9) with the corresponding data for hemicalide does not support the 31,32-*anti* configuration.

Scheme 2 Synthesis of the C29–C34 alkene and fragment union. Reagents and conditions: (a) *cis*-but-2-ene, *t*BuOK, *n*BuLi, THF, −78 → −45 °C; (+)-Ipc$_2$BOMe, −78 °C; BF$_3$·OEt$_2$; **19**, THF, −78 °C; H$_2$O$_2$, NaOH, −78 °C → rt; (b) TBSOTf, 2,6-lutidine, CH$_2$Cl$_2$, −78 °C, 88% over two steps, >20:1 dr; (c) BH$_3$·SMe$_2$, THF, 0 °C → rt; H$_2$O$_2$, NaOH, MeOH, 0 °C → rt, 80%; (d) (COCl)$_2$, DMSO; Et$_3$N, CH$_2$Cl$_2$, −78 °C → rt; (e) MePPh$_3$Br, *n*BuLi, THF, 0 °C → rt, 60% over two steps; (f) Hoveyda–Grubbs II Catalyst (13 mol%), *p*-benzoquinone, PhMe, 80 °C; (g) DDQ, CH$_2$Cl$_2$/pH 9.2 buffer (4:1), 0 °C → rt, 59% over two steps; (h) aq. HF/MeCN (10%), −20 °C; Et$_3$N, 99%.

NMR spectroscopic comparison with the corresponding region for the hemicalide spectra (CD$_3$OD) processed in-house could now be conducted (Table 2 and Fig. 4). Initial inspection revealed that all the 31,32-*syn* diastereomers (entries 1 to 3, $\Sigma|\Delta_H| < 0.11$ ppm; $\Sigma|\Delta_C| < 2.86$ ppm) possessed a much lower chemical shift deviation relative to hemicalide compared with the 31,32-*anti* configuration previously reported (entry 4: $\Sigma|\Delta_H| = 0.33$ ppm; $\Sigma|\Delta_C| = 8.48$ ppm).[9] This strongly supported the assignment of a 31,32-*syn* configuration in the natural product. Next, a comparison of the ^{13}C NMR data for fragments **2c** (42,45-*syn*) and **2b** (42,45-*anti*) with hemicalide supported the 42,45-*anti* configuration assigned above (entry 2: $\Sigma|\Delta_C| = 2.72$ ppm) over the alternative 42,45-*syn* isomer (entry 3: $\Sigma|\Delta_C| = 2.86$ ppm). A final comparison of 32,36-*syn* **2b** (entry 2), 32,36-*anti* **2a** (entry 1) and the hemicalide ^{1}H and ^{13}C NMR data conclusively gave lower chemical shift deviations for the 32,36-*anti* diastereomer (entry 1: $\Sigma|\Delta_H| = 0.06$ ppm; $\Sigma|\Delta_C| = 1.57$ ppm) over the alternative 32,36-*syn* isomer (entry 2: $\Sigma|\Delta_H| = 0.11$ ppm; $\Sigma|\Delta_C| = 2.72$ ppm), representing the best fit candidate for future targeted synthetic efforts. Importantly, this provides strong evidence for the relative configurational assignment of the C31, C32 and C45 stereocentres.

In summary, we have developed a streamlined synthesis of the C29–C46 region of hemicalide, enabling the flexible installation of both the C45 hydroxyl and the C31–C32 stereocluster to give candidate structural permutations.

Table 2 Statistical summary of absolute errors $|\Delta|$ (ppm)^{ab} for each diastereomer compared to the reported NMR spectra (ref. 1) of hemicalide (**1**)

Entry	Sum $|\Delta|$ ^{1}H	Max $|\Delta|$ ^{1}H	Sum $|\Delta|$ ^{13}C	Max $|\Delta|$ ^{13}C
1. 31,32-*syn*, 32,36-*anti*, 42,45-*anti* 2a	**0.06**	**0.04**	**1.57**	**0.81**
2. 31,32-*syn*, 32,36-*syn*, 42,45-*anti* **2b**	0.11	0.04	2.72	0.72
3. 31,32-*syn*, 32,36-*syn*, 42,45-*syn* **2c**	0.10	0.03	2.86	0.73
4. Lecourt *et al.* diastereomer (ref. 9), 31,32-*anti*, 32,36-*syn*, 42,45-*anti*	0.33	0.14	8.48	1.32

^{a} Absolute errors taken for ^{1}H and ^{13}C NMR chemical shifts between H/C31-H/C46. ^{b} $|\Delta|$ = δ(experimental shift) – δ(reported shift), errors in ppm.
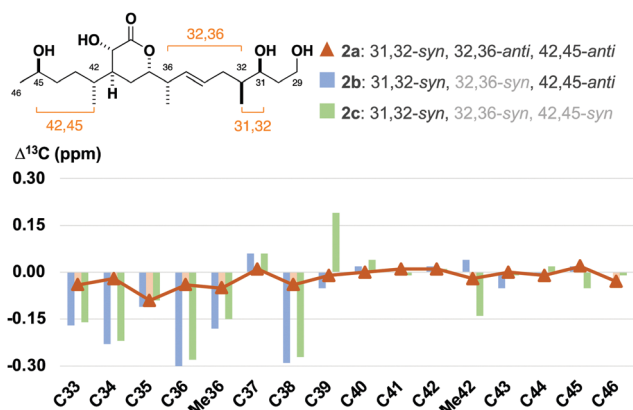
Fig. 4 Bar graph highlighting the ^{13}C NMR chemical shift differences between the C33–C46 diastereomers **2a**, **2b** and **2c** relative to hemicalide (**1**), overlaid with a line graph for the best match in **2a**. See the ESI† for expanded bar graphs and detailed tabulated data.

Spectroscopic comparison with each diastereomer then provided firm evidence in support of the (i) 31,32-*syn*, (ii) 32,36-*anti* and (iii) 42,45-*anti* configuration. In conjunction with the prior assignment of the C1–C24 region,[7] this serves to reduce the stereochemical conundrum to only eight possible candidate diastereomers (out of >1 million). In addition to reaffirming the undisputed power of chemical synthesis as the arbiter of stereochemical determination,[25–27] the current work should enable future access to advanced intermediates towards interrogating a now-tractable set of possible diastereomers within the vast stereochemical space occupied by hemicalide.

Conflicts of interest

There are no conflicts to declare.

Notes and references

1 (*a*) I. Carletti, C. Debitus and G. Massiot, *Molécules polykétides comme agents anticancéreux*, *Pat. Appl. Pub.*, WO2011051380A1 (FR), 2011; (*Chem. Abstr.*, 2011, **154**, 5130950); (*b*) L. Marcourt and G. Massiot, *Eur. J. Org. Chem.*, 2022, e22020208.
2 E. Fleury, M.-I. Lannou, O. Bistri, F. Sautel, G. Massiot, A. Pancrazi and J. Ardisson, *J. Org. Chem.*, 2009, **74**, 7034.
3 S. G. Smith and J. M. Goodman, *J. Am. Chem. Soc.*, 2010, **132**, 12946.
4 C. I. MacGregor, B. Y. Han, J. M. Goodman and I. Paterson, *Chem. Commun.*, 2016, **52**, 4632.
5 S. Specklin, G. Boissonnat, C. Lecourt, G. Sorin, M.-I. Lannou, J. Ardisson, F. Sautel, G. Massiot, C. Meyer and J. Cossy, *Org. Lett.*, 2015, **17**, 2446.
6 E. De Gussem, W. Herrebout, S. Specklin, C. Meyer, J. Cossy and P. Bultinck, *Chem. – Eur. J.*, 2014, **20**, 17385.
7 B. Y. Han, N. Y. S. Lam, C. I. MacGregor, J. M. Goodman and I. Paterson, *Chem. Commun.*, 2018, **54**, 3247.
8 C. Lecourt, S. Boinapally, S. Dhambri, G. Boissonnat, C. Meyer, J. Cossy, F. Sautel, G. Massiot, J. Ardisson, G. Sorin and M.-I. Lannou, *J. Org. Chem.*, 2016, **81**, 12275.
9 C. Lecourt, S. Dhambri, K. Yamani, G. Boissonnat, S. Specklin, E. Fleury, K. Hammad, E. Auclair, S. Sablé, A. Grondin, P. B. Arimondo, F. Sautel, G. Massiot, C. Meyer, J. Cossy, G. Sorin, M. I. Lannou and J. Ardisson, *Chem. – Eur. J.*, 2019, **25**, 2745.
10 G. Sorin, E. Fleury, C. Tran, E. Prost, N. Molinier, F. Sautel, G. Massiot, S. Specklin, C. Meyer, J. Cossy, M. I. Lannou and J. Ardisson, *Org. Lett.*, 2013, **15**, 4734.
11 N. Y. S. Lam and I. Paterson, *Eur. J. Org. Chem.*, 2020, 2310.
12 K. C. Nicolaou and S. A. Snyder, *Angew. Chem., Int. Ed.*, 2005, **44**, 1012.
13 M. J. Anketell, T. M. Sharrock and I. Paterson, *Angew. Chem., Int. Ed.*, 2020, **59**, 1572.
14 I. Paterson and K.-S. Yeung, *Tetrahedron Lett.*, 1993, **34**, 5347.
15 I. Paterson, J. M. Goodman, M. A. Lister, R. C. Schumann, C. K. McClure and R. D. Norcross, *Tetrahedron*, 1990, **46**, 4663.
16
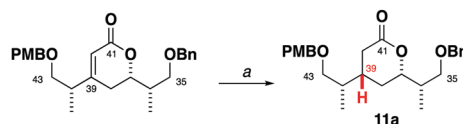
Copper hydride-mediated conjugate reduction of the corresponding α,β-unsaturated δ-lactone gave exclusively the 39-*epi* lactone **11a**. (a) (BDP)CuH (10 mol%), PMHS, PPh₃, PhMe, 50 °C, 60%. B. A. Baker, Z. V. Bošković and B. H. Lipschutz, *Org. Lett.*, 2008, **10**, 289.

17 I. Wang, T. J. Chen, K. J. Chaa, T. C. J. Tsai, G. Lohaus, L. Friedman, H. Shechter, J. M. Brown, R. G. Naik, S. A. Hall, R. H. Crabtree, M. W. Davis, G. Stork and D. E. Kahne, *J. Org. Chem.*, 2002, **51**, 2655.
18 F. A. Davis, L. C. Vishwakarma, J. M. Billmers and J. Finn, *J. Org. Chem.*, 1984, **49**, 3241.
19 I. Paterson, K.-S. Yeung and J. B. Smaill, *Synlett*, 1993, 774.
20 S. Terashima, N. Tanno and K. Koga, *J. Chem. Soc., Chem. Commun.*, 1980, 1026.
21 I. Paterson and M. Tudge, *Angew. Chem., Int. Ed.*, 2003, **42**, 343.
22 H. C. Brown, P. K. Jadhav and K. S. Bhat, *J. Am. Chem. Soc.*, 1988, **110**, 1535.
23 M. J. Anketell, T. M. Sharrock and I. Paterson, *Org. Biomol. Chem.*, 2020, **18**, 8109.
24 J. Wu, P. Lorenzo, S. Zhong, M. Ali, C. P. Butts, E. L. Myers and V. K. Aggarwal, *Nature*, 2017, **547**, 436.
25 T. P. Stockdale, N. Y. S. Lam, M. J. Anketell and I. Paterson, *Bull. Chem. Soc. Jpn.*, 2021, **94**, 713.
26 N. Y. S. Lam, T. P. Stockdale, M. J. Anketell and I. Paterson, *Chem. Commun.*, 2021, **57**, 3171.
27 N. Y. S. Lam, G. Muir, V. R. Challa, R. Britton and I. Paterson, *Chem. Commun.*, 2019, **55**, 9717.